Molecular properties of the N-terminal extension of the fission yeast kinesin-5, Cut7

M. Edamatsu

Department of Life Sciences, Graduate School of Arts and Sciences,
the University of Tokyo, Meguro-ku, Tokyo, Japan

Corresponding author: M. Edamatsu
E-mail: cedam@mail.ecc.u-tokyo.ac.jp

ABSTRACT. Kinesin-5 plays an essential role in spindle formation and function, and serves as a potential target for anti-cancer drugs. The aim of this study was to elucidate the molecular properties of the N-terminal extension of the *Schizosaccharomyces pombe* kinesin-5, Cut7. This extension is rich in charged amino acids and predicted to be intrinsically disordered. In *S. pombe* cells, a Cut7 construct lacking half the N-terminal extension failed to localize along the spindle microtubules and formed a monopolar spindle. However, a construct lacking the entire N-terminal extension exhibited normal localization and formed a typical bipolar spindle. In addition, *in vitro* analyses revealed that the truncated Cut7 constructs demonstrated similar motile velocities and directionalities as the wild-type motor protein, but the microtubule landing rates were significantly reduced. These findings suggest that the N-terminal extension is not required for normal Cut7 intracellular localization or function, but alters the microtubule-binding properties of this protein *in vitro*.

Key words: *Schizosaccharomyces pombe*; Mitosis; Cytoskeleton; Cell motility; Spindle; TIRF assay

INTRODUCTION

Kinesin is an adenosine triphosphate (ATP)-dependent molecular motor that moves along microtubules. The kinesin superfamily is divided into 14 subfamilies that play various roles in intracellular transport and cytoskeletal reorganization (Miki et al., 2005). Most kinesin members, with the exception of kinesin-13 and -14, have a conserved N-terminal motor domain and move toward the plus end of microtubules (Miki et al., 2005).

Kinesin-5 is a mitotic kinesin and constitutes a potential target for anti-cancer drugs owing to its essential role in mitosis. This protein crosslinks and slides apart antiparallel spindle microtubules via plus-end-directed motility (Saunders and Hoyt, 1992). The microtubule-binding properties of kinesin-5 change greatly during cell division, and are regulated by Cdk1 kinase in *Xenopus* (Sawin and Mitchison, 1995) and *Drosophila* cells (Sharp et al., 1999). Moreover, the motor activity of kinesin-5 is antagonized by minus-end-directed motors, such as kinesin-14, during mitosis (Saunders and Hoyt, 1992).

Kinesin-5 comprises a conserved motor domain and a divergent stalk-tail region (Miki et al., 2005). The former hydrolyzes ATP to produce the force required to slide microtubules. Of the latter, the stalk forms a coiled-coil structure and is responsible for bipolar tetramer formation, while the tail binds to microtubules in an ATP-independent manner to maintain crosslinks (Weinger et al., 2011). In addition, kinesin-5 from lower eukaryotes contains a distinct extension at the N-terminus of the motor domain. The N-terminal extension of the fungal kinesin-5 BimC binds to microtubules *in vitro* (Stock et al., 2003), but its contribution to the motor activity and intracellular function of this protein is unknown.

Cut7, fission yeast kinesin-5, is implicated in spindle formation and function (Hagan and Yanagida, 1990). It is diffusely distributed in the nucleus during interphase and concentrated at spindle poles during mitosis. Early in mitosis, Cut7 localizes along spindle microtubules, from which it is gradually depleted in later stages (Fu et al., 2009). Cut7 loss-of-function mutants display abnormal, monopolar spindles and fail to complete mitosis (Hagan and Yanagida, 1990). Given its mitotic function in sliding spindle microtubules to separate poles, Cut7 was considered a plus-end-directed motor, similar to other kinesin-5 family members. However, a recent report revealed that Cut7 moves toward both the minus and plus ends of microtubules (Edamatsu, 2014), as with budding yeast kinesin-5 (Roostalu et al., 2011; Fridman et al., 2013). Furthermore, it was recently shown that Cut7 regulates the microtubule-nucleating activity of the γ-tubulin ring complex (γ-TuRC) at spindle poles through an antagonistic relationship with pkl1 (fission yeast kinesin-14; Olmsted et al., 2014). As the properties of the Cut7 motor are of current interest, this study aimed to investigate the molecular characteristics of the N-terminal extension of this protein using *in vivo* and *in vitro* analyses.

MATERIAL AND METHODS

Bioinformatic analysis

N-terminal extension amino acid sequences were aligned using ClustalW (http://www.genome.jp/tools/clustalw/). For estimation of intrinsic disorder, six of seven prediction programs available for the kinesin superfamily (Seeger and Rice, 2013) were used in this study: GlobPlot (http://globplot.embl.de/); DisEMBL (http://dis.embl.de/); DISOPRED2 (http://bioinf.cs.ucl.ac.uk/disopred/); IUPred (http://iupred.enzim.hu/); DISpro (http://scratch.proteomics.ics.uci.edu/); and OnD-CRF (http://babel.ucmp.umu.se/ond-crf). The DRIP-PRED web server was not available at the time of investigation.

Construction of recombinant *Schizosaccharomyces pombe* strains

S. pombe cells were grown in 0.5% yeast extract and 3% dextrose or synthetic complete medium with appropriate supplements. Genetic analyses of *S. pombe* were performed as previously described (Moreno et al., 1991).

The integration plasmids used for the *in vivo* analysis are shown in **Figure S1**. First, the endogenous *cut7* promoter in the parental strain was replaced with the inducible *nmt81* promoter using *Sma*I-digested pFA6a-*nmt81-cut7*. Truncated Cut7-3xgreen fluorescent protein (GFP) and mCherry-Atb2 expression cassettes were then integrated into the *ade-* locus of the parental strain using *Bam*HI-digested pBS-*atb2-cut7*.

Western blotting

Total cell extracts were prepared essentially as described in Moreno et al. (1991). Proteins were electrophoresed on a polyacrylamide gel and transferred to a polyvinylidene fluoride membrane. After incubating the membrane with polyclonal anti-GFP antibody (BD Biosciences, San Jose, CA, USA), antigens were detected using an alkaline phosphatase-conjugated secondary antibody (KPL, Gaithersburg, MD, USA) and a Phosphatase Substrate System kit (KPL).

Construction and preparation of recombinant proteins

For *in vitro* analyses, Cut7-ΔN1 (amino acids 46-1085) and Cut7-ΔN2 (amino acids 70-1085) sequences were amplified by polymerase chain reaction and cloned into the pCold-GFP vector (Edamatsu, 2014). Cut7-wt-GFP-his6 (amino acids 1-1085) and rat kinesin-1-GFP-his6 (amino acids 1-430) have been described previously (Edamatsu, 2014). These constructs were expressed in *Escherichia coli* cells and prepared as explained in a prior publication (Edamatsu, 2014).

In vitro analyses

The total internal reflection fluorescence (TIRF) assay was performed as previously reported (Edamatsu, 2014). The direction of truncated Cut7 construct motion was determined by application of excess rat kinesin-1-GFP after the movement of Cut7 had been recorded. Directions were determined from 15-20 microtubules on which Cut7 and kinesin-1 spots were seen to move. Motile velocity (drift velocity) was determined from mean square displacement plots of Cut7 spots, as previously described (Furuta et al., 2008).

The landing assay (Soppina and Verhey, 2014) was slightly modified in this study. Briefly, the flow chamber was filled with assay solution containing 10 mM piperazine-*N,N'*-bis(2-ethanesulfonic acid), pH 7.0, 200 mM potassium acetate, 4 mM MgSO$_4$, 1 mM ethylene glycol tetraacetic acid, 1 mM dithiothreitol, 1 mM ATP, 10 μM paclitaxel, 1 mg/mL dephosphorylated casein (Sigma-Aldrich, Tokyo, Japan), 1 to 100 pM Cut7-GFP, 0.1% glucose (w/w), 43 U/mL glucose oxidase (Sigma-Aldrich), and 650 U/mL catalase (Roche, Tokyo, Japan), and fluorescent images were captured at 7 frames per second. The number of Cut7 spots landing on all Cy5-labeled microtubules in the microscope field of view was counted and then divided by the total length of microtubules, recording duration, and protein concentration to obtain a landing rate expressed in units of landing events·μm^{-1}·min^{-1}·nM^{-1}.

RESULTS

Bioinformatic analysis of the kinesin-5 N-terminal extension

Kinesin-5 in lower eukaryotes has a divergent extension consisting of approximately 70 amino acids at the N-terminus of the motor domain. This extension is rich in charged amino acids (Figure 1A and B), which is characteristic of intrinsically disordered (ID) proteins. ID proteins or regions are broadly defined as those that do not fold into stable secondary structures under physiological conditions. This attribute is thought to accelerate interactions with binding partners (Oldfield and Dunker, 2014).

Recent reports using the GlobPlot, DisEMBL, DISOPRED2, IUPred, DISpro, OnD-CRF, and DRIP-PRED programs have predicted ID regions in all human kinesin superfamily members (Seeger and Rice, 2013). Thus, the N-terminal extension of Cut7 was analyzed using these prediction tools in this investigation. Figure 1C presents results obtained using the DISOPRED2 program, which returned a high ID region score for the Cut7 N-terminal extension, in contrast to the motor domain. All other available programs indicated higher ID region probabilities than the designated thresholds with respect to this extension. In addition, the N-terminal extensions of other kinesin-5 members, such as Cin8 and BimC, displayed prediction profiles similar to that of Cut7 (Figure 1D and E).

Figure 1. Bioinformatic analysis of the N-terminal extension of kinesin-5. **A.** Kinesin-5 domain structures. aa = amino acids. **B.** Amino acid sequence alignment of kinesin-5 N-terminal extensions, including those from *Homo sapiens* (*Hs*Eg5), *Drosophila melanogaster* (*Dm*KLP61F), *Aspergillus nidulans* (*An*BimC), *Saccharomyces cerevisiae* (*Sc*Cin8), and *Schizosaccharomyces pombe* (*Sp*Cut7). Basic and acidic amino acids are colored green and red, respectively. **C.** Intrinsic disorder in the N-terminal extension and motor domain of Cut7 (1-427 aa) predicted by the DISOPRED2 program. The corresponding regions of **D.** Cin8 (1-522 aa) and **E.** BimC (1-423 aa) were also analyzed.

In vivo analyses of truncated Cut7 constructs

In vivo properties of the Cut7 N-terminal extension were examined using truncated mutants. The N- and C-terminal halves of the extension are rich in basic and acidic amino acids, respectively. Therefore, Cut7-wt (wild-type), Cut7-ΔN1 (lacking the N-terminal half of the extension), and Cut7-ΔN2 (lacking the entire extension) constructs were examined in this study (Figure 2A). These constructs were fused with 3xGFP at the C-terminus for intracellular visualization, as Cut7-3xGFP is known to retain its function in *S. pombe* cells (Fu et al., 2009).
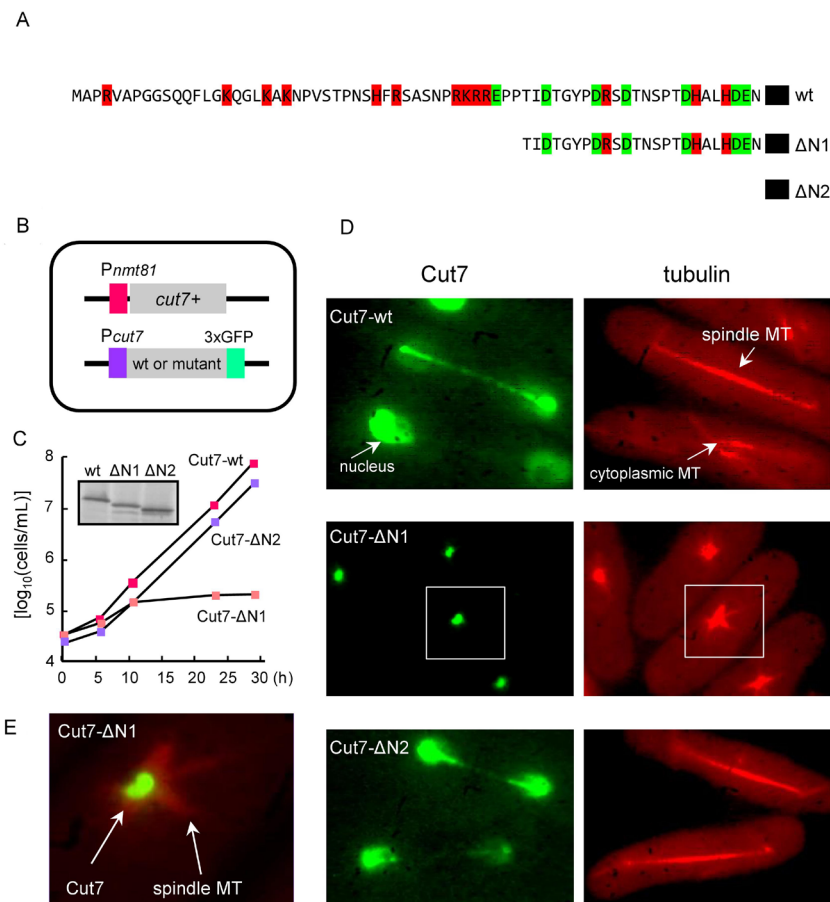
Figure 2. *In vivo* analyses of the Cut7 N-terminal extension. **A.** N-terminal sequences of the Cut7 constructs used in this study. Basic and acidic amino acids are colored green and red, respectively. wt = wild type. **B.** Schematic representation of the *in vivo* analysis. Phenotypes of the Cut7 mutants were examined after shutting off the *nmt81* promoter. GFP = green fluorescent protein. **C.** Growth curves of the Cut7 mutants. Cell concentrations were determined at different time points after shutting off the *nmt81* promoter by adding thiamine to the culture medium. Expression of Cut7 constructs was examined by western blot analysis using an anti-GFP antibody (inset). Each lane contained equal amounts of total protein. **D**. Localization of Cut7 constructs. Fluorescence micrographs of Cut7-3xGFP (left panels) and mCherry-tubulin (right panels) are shown. The scale bar represents 5 μm. MT = microtubule. **E.** Enlarged view of area outlined in panel D. Merged image of Cut7 (green) and microtubule (red) localization. The *in vivo* assay was performed in triplicate and representative fluorescence micrographs are shown.

The experiment is outlined in Figure 2B. Because the *cut7* gene is essential for cell viability, a modified shutoff experiment was performed. Firstly, the endogenous *cut7* promoter was replaced with the inducible *nmt81* promoter by homologous recombination (Figure 2B and **Figure S1**). This parental strain formed monopolar spindles similar to the Cut7 loss-of-function mutant following shutoff of the *nmt81* promoter. Each Cut7 construct expression cassette was then inserted into the *ade-* locus of the parental strain (Figure 2B and **Figure S1**), and microtubules were visualized using mCherry-Atb2. Expression of the Cut7 constructs is shown in Figure 2C (inset).

First, the growth of these truncated N-terminal extension mutants was examined. Cut7-ΔN1 cells did not grow once the *nmt81* promoter had been shut off, whereas Cut7-ΔN2 cells grew normally under the same culture conditions (Figure 2C). Localization of the Cut7 constructs and tubulin is shown in Figure 2D. Cut7-ΔN1 cells formed monopolar spindles similar to those found in the Cut7 loss-of-function mutant, and displayed Cut7 localization at spindle poles but not along spindle microtubules (Figure 2D and E). In contrast, Cut7-ΔN2 cells formed normal bipolar spindles, and exhibited Cut7 localization similar to that of Cut7-wt cells (Figure 2D). These findings suggest that the N-terminal extension of Cut7 is not required for localization along spindle microtubules or at spindle poles. However, truncation of its N-terminal half can alter Cut7 spindle microtubule localization.

In vitro analyses of truncated Cut7 constructs

To further examine the molecular properties of the Cut7 N-terminal extension, the truncated constructs were characterized using *in vitro* analyses. These constructs were fused with 1xGFP at their C-termini and individual Cut7 spots were observed on Cy5-labeled microtubules by TIRF microscopy (Figure 3A). Cut7-ΔN1 and Cut7-ΔN2 constructs were found to move toward the minus ends of microtubules at velocities similar to that of Cut7-wt (Figure 3B and C).
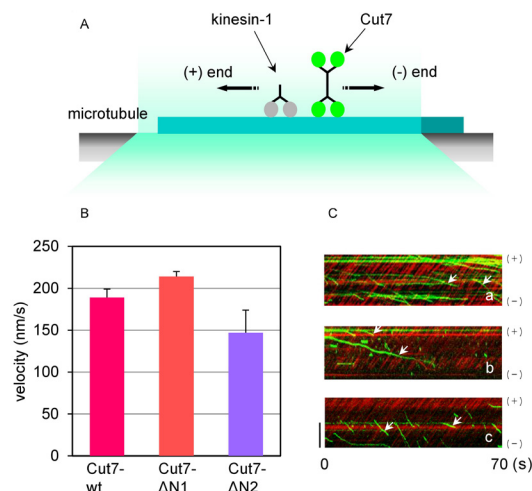

Figure 3. Motile properties of the truncated Cut7 constructs. **A.** Schematic representation of the total internal reflection fluorescence (TIRF) assay. **B.** Motile velocities of the truncated Cut7 constructs calculated from mean square displacement plots of Cut7 spots, as previously described (Furuta et al., 2008). Values were determined from three independent experiments. Error bars represent the standard error of the mean. **C.** TIRF assay kymographs showing direction of movement of the truncated Cut7 constructs. Motion direction was determined by application of excess rat kinesin-1-GFP after movement of (a) Cut7-wt, (b) Cut7-ΔN1, and (c) Cut7-ΔN2 constructs had been recorded. Cut7 (green) and kinesin-1 (red) signals are merged. Arrows indicate movement of Cut7 motors. The scale bar represents 2 μm.

Figure 4B shows representative fluorescent images of Cut7 proteins on microtubules, indicating a reduced presence of the two truncated constructs compared to the Cut7-wt form. The landing rates of the Cut7-ΔN1 and Cut7-ΔN2 constructs on microtubules, determined using TIRF microscopy (Figure 4A), were approximately one-sixtieth and one-eighth that of Cut7-wt, respectively (Figure 4C). These findings indicate that the N-terminal extension alters the landing rate of Cut7 on microtubules but has little effect on motile velocity and directionality *in vitro*.
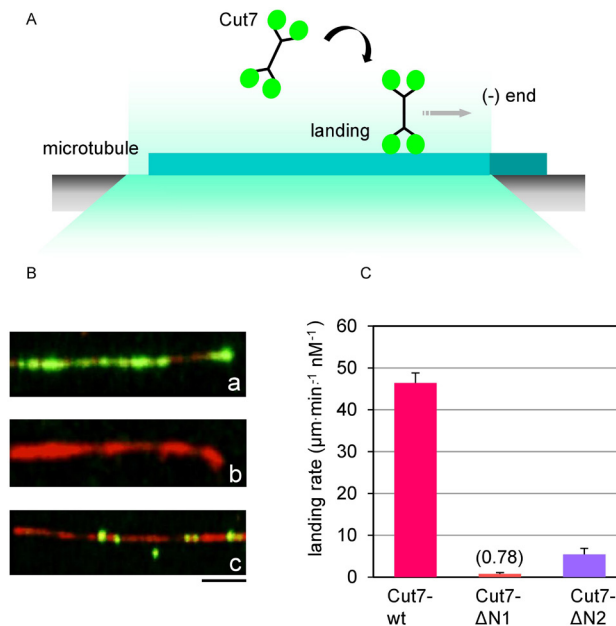
Figure 4. Landing assay of the truncated Cut7 constructs. **A.** Schematic representation of the landing assay. **B.** Representative fluorescence micrographs of (a) Cut7-wt, (b) Cut7-ΔN1, and (c) Cut7-ΔN2 constructs on microtubules. Cut7 and microtubules are indicated in green and red, respectively. The scale bar represents 2 μm. **C.** Landing rates of the Cut7 constructs on microtubules, determined from three independent experiments. Error bars represent the standard error of the mean.

DISCUSSION

This study characterized the molecular properties of the N-terminal extension of Cut7. This is expected to be a region of ID, based on results obtained from protein prediction programs. ID was also identified in the N-terminal extensions of other kinesin-5 members, such as Cin8 and BimC. The absence of a static structure may be a common feature of such kinesin-5 extensions. In general, ID proteins recognize multiple partners due to their structural flexibility, and are susceptible to post-translational modifications (Oldfield and Dunker, 2014). However, no modifications or binding partners other than microtubules have been reported for kinesin-5 N-terminal extensions to date.

In vitro analyses revealed that the N-terminal extension alters the landing rate of Cut7 on microtubules. Certain basic regions in kinesin motors are associated with the E-hook, an acidic region at the C-terminus of tubulin. In the KIF1A motor, the K-loop, a positively charged loop rich in lysine, binds to the E-hook and enhances the binding affinity of KIF1A to microtubules (Okada and Hirokawa, 2000). The theoretical isoelectric point of the entire Cut7 extension has been calculated

to be 9.81, which is assumed to be basic in the assay buffer. This may result in the wild-type protein having an increased landing rate compared to the ΔN2 construct lacking the extension. In addition, the theoretical isoelectric points of the N- and C-terminal halves of the extension are 12.2 and 4.16, respectively, suggesting that the landing rate of Cut7-ΔN1 lacking the basic region of the N-terminal extension should be reduced.

These observations appear to be consistent with the phenotypes induced by Cut7-ΔN1 and Cut7-ΔN2 *in vivo*. The ΔN1 construct, which exhibited a low landing rate *in vitro*, did not localize along spindle microtubules and formed abnormal, monopolar spindles. In contrast, the ΔN2 form, which demonstrated a higher landing rate, did not result in the defects noted in cells expressing Cut7-ΔN1. Kinesin-5 shows highly dynamic behavior on spindle microtubules, and its half-life along these structures is considerably reduced compared with that at the spindle poles (Uteng et al., 2008). Thus, it is likely that the low landing rate of Cut7-ΔN1 enhances its depletion on spindle microtubules and induces monopolar spindle formation.

In vivo analyses also indicate that the N-terminal extension is not involved in Cut7 localization at spindle poles. A recent report revealed that Cut7 regulates microtubule nucleation at spindle poles, and that its head and tail bind to the γ-TuRC (Olmsted et al., 2014). Considering the localization of Cut7-ΔN2, the N-terminal extension is unlikely to be involved in such γ-TuRC binding. The mechanism by which microtubule nucleation at spindle poles is regulated is thought to be conserved in human cells (Olmsted et al., 2014), and thus Eg5 (human kinesin-5) might associate with the γ-TuRC in a similar manner to Cut7.

The microtubule-binding properties of Cut7 are thought to change in a cell cycle-dependent manner. During early mitosis, Cut7 is localized along spindle microtubules, but in late mitosis is only found near the spindle poles (Fu et al., 2009). A recent report revealed that Cut7 is not important for spindle elongation in anaphase B and that Klp9, fission yeast kinesin-6, is involved in such elongation at the spindle midzone (Fu et al., 2009). The localization of Klp9 is dependent on Ase1, a fission yeast microtubule-bundling protein whose activity is regulated by the Cdk1-Clp1 system (Fu et al., 2009). Cut7 contains a putative Cdk1-phosphorylation site in the BimC box present in its tail, but this site is not functional *in vivo*. In addition, the N-terminal extension of Cut7 contains two more such sites; however, these do not appear to be implicated in its intracellular localization considering the Cut7-ΔN2 phenotype. The mechanism by which the microtubule-binding properties of Cut7 are regulated during different cell-cycle phases would be an interesting subject for future investigation.

Conflicts of interest

The author declares no conflict of interest.

REFERENCES

Edamatsu M (2014). Bidirectional motility of the fission yeast kinesin-5, Cut7. *Biochem. Biophys. Res. Commun.* 446: 231-234. http://dx.doi.org/10.1016/j.bbrc.2014.02.106

Fridman V, Gerson-Gurwitz A, Shapira O, Movshovich N, et al. (2013). Kinesin-5 Kip1 is a bi-directional motor that stabilizes microtubules and tracks their plus-ends *in vivo. J. Cell Sci.* 126: 4147-4159.http://dx.doi.org/10.1242/jcs.125153

Fu C, Ward JJ, Loiodice I, Velve-Casquillas G, et al. (2009). Phospho-regulated interaction between kinesin-6 Klp9p and microtubule bundler Ase1p promotes spindle elongation. *Dev. Cell* 17: 257-267. http://dx.doi.org/10.1016/j.devcel.2009.06.012

Furuta K, Edamatsu M, Maeda Y and Toyoshima YY (2008). Diffusion and directed movement: *in vitro* motile properties of fission yeast kinesin-14 Pkl1. *J. Biol. Chem.* 283: 36465-36473.http://dx.doi.org/10.1074/jbc.M803730200

Hagan I and Yanagida M (1990). Novel potential mitotic motor protein encoded by the fission yeast cut7+ gene. *Nature* 347: 563-566.http://dx.doi.org/10.1038/347563a0

Miki H, Okada Y and Hirokawa N (2005). Analysis of the kinesin superfamily: insights into structure and function. *Trends Cell Biol.* 15: 467-476.http://dx.doi.org/10.1016/j.tcb.2005.07.006

Moreno S, Klar A and Nurse P (1991). Molecular genetic analysis of fission yeast *Schizosaccharomyces pombe. Methods Enzymol.* 194: 795-823.http://dx.doi.org/10.1016/0076-6879(91)94059-L

Okada Y and Hirokawa N (2000). Mechanism of the single-headed processivity: diffusional anchoring between the K-loop of kinesin and the C terminus of tubulin. *Proc. Natl. Acad. Sci. USA* 97: 640-645.http://dx.doi.org/10.1073/pnas.97.2.640

Oldfield CJ and Dunker AK (2014). Intrinsically disordered proteins and intrinsically disordered protein regions. *Annu. Rev. Biochem.* 83: 553-584.http://dx.doi.org/10.1146/annurev-biochem-072711-164947

Olmsted ZT, Colliver AG, Riehlman TD and Paluh JL (2014). Kinesin-14 and kinesin-5 antagonistically regulate microtubule nucleation by γ-TuRC in yeast and human cells. *Nat. Commun.* 5: 5339.http://dx.doi.org/10.1038/ncomms6339

Roostalu J, Hentrich C, Bieling P, Telley IA, et al. (2011). Directional switching of the kinesin Cin8 through motor coupling. *Science* 332: 94-99.http://dx.doi.org/10.1126/science.1199945

Saunders WS and Hoyt MA (1992). Kinesin-related proteins required for structural integrity of the mitotic spindle. *Cell* 70: 451-458.http://dx.doi.org/10.1016/0092-8674(92)90169-D

Sawin KE and Mitchison TJ (1995). Mutations in the kinesin-like protein Eg5 disrupting localization to the mitotic spindle. *Proc. Natl. Acad. Sci. USA* 92: 4289-4293.http://dx.doi.org/10.1073/pnas.92.10.4289

Seeger MA and Rice SE (2013). Intrinsic Disorder in the Kinesin Superfamily. *Biophys. Rev.* 5. http://dx.doi.org/10.1007/s12551-012-0096-5

Sharp DJ, McDonald KL, Brown HM, Matthies HJ, et al. (1999). The bipolar kinesin, KLP61F, cross-links microtubules within interpolar microtubule bundles of *Drosophila* embryonic mitotic spindles. *J. Cell Biol.* 144: 125-138. http://dx.doi.org/10.1083/jcb.144.1.125

Soppina V and Verhey KJ (2014). The family-specific K-loop influences the microtubule on-rate but not the superprocessivity of kinesin-3 motors. *Mol. Biol. Cell* 25: 2161-2170.http://dx.doi.org/10.1091/mbc.E14-01-0696

Stock MF, Chu J and Hackney DD (2003). The kinesin family member BimC contains a second microtubule binding region attached to the N terminus of the motor domain. *J. Biol. Chem.* 278: 52315-52322. http://dx.doi.org/10.1074/jbc.M309419200

Uteng M, Hentrich C, Miura K, Bieling P, et al. (2008). Poleward transport of Eg5 by dynein-dynactin in *Xenopus laevis* egg extract spindles. *J. Cell Biol.* 182: 715-726.

Weinger JS, Qiu M, Yang G and Kapoor TM (2011). A nonmotor microtubule binding site in kinesin-5 is required for filament crosslinking and sliding. *Curr. Biol.* 21: 154-160.http://dx.doi.org/10.1016/j.cub.2010.12.038

Supplementary Material

Figure S1. Schematic representation of the integration vectors used in this study. NTR = nontranslated region, GFP = green fluorescent protein.

http://www.geneticsmr.com/year2016/vol15-1/pdf/gmr7799_supplementary.pdf